[Journal of Geophysical Research: Atmospheres]

Supporting Information for

Ice core $\delta^{18}O$ record linked to Western Arctic sea ice variability

Stacy E. Porter[1], Ellen Mosley-Thompson[1, 2], and Lonnie G. Thompson[1, 3]

[1]Byrd Polar and Climate Research Center, The Ohio State University, Columbus, Ohio, 43210, USA

[2]Department of Geography, Atmospheric Sciences Program, The Ohio State University

[3]School of Earth Sciences, The Ohio State University

Contents of this file

Introduction

The supporting information includes a more detailed description of the analysis and timescale development for the Bona-Churchill ice core and analysis of the isotope-enabled models. Much of the main text of the manuscript focuses on the relationship between the Bona-Churchill (B-C) isotopic record and Western Arctic climate during the spring season, thus the analyses for the remaining seasons are provided here.

Text S1. Analysis and dating the B-C ice core

No meteorological observations are available from the B-C col, but the average surface temperature can be estimated from the borehole temperatures. For sites like B-C which are dry (very few thin (~1 mm) melt layers were observed) and cold the temperature at 10 to 15 m depth provides a reasonable estimate of the mean annual air temperature (Cuffey and Paterson, 2010). The temperature at 10 m in the borehole was -23.1^{0}C and -6^{0}C at the ice-bedrock contact indicating that the basal ice is frozen to the bed.

The entire length (460.96 m) of the B-C core was cut into three sets of 12,161 discrete co-registered samples each. The initial sample size is typically determined using the depth of the 1963 Beta radioactivity peak to calculate the sample size that is required to cut 10 to 15 samples per estimated annual layer thickness. The sample size for the upper 10 m was 0.115 m, 0.106 m from 20 to 50 m and it was slowly decreased to 0.016 m from 430 to 460.96 m. The three sets of samples were analyzed for (1) the concentrations and size distributions of insoluble dust particles (0.63 μm ≤ diameter < 20 μm) using a Coulter Counter TAII; (2) the oxygen ($\delta^{18}O$) and hydrogen (δD) isotopic compositions using a Finnigan-MAT Delta Plus mass spectrometer with analytical precisions of 0.2 and 2.0 ‰, respectively; and (3) the concentrations of major anions and cations using a Dionex ICS-2500 ion chromatograph with a Dionex AS 40 auto sampler. All sample handling and analyses for dust and ionic concentrations were conducted in a Class 100 clean room, and these analyses were conducted in 2002 and 2003. Urmann (2009) found the δD data to be intermittently inconsistent, particularly prior to 1880 CE or below ~182 m. He suspected that drilling fluid (an ethanol and water mixture) used during thermal drilling may have contaminated the ice along internal microfractures. He estimated that the percent of usable samples dropped as low as 70% by 1800 CE and thus, the δD and d-excess data for this core have not been published. The Beta radioactivity was measured using a Tennelec LB 1000 series alpha/beta counter.

The individual years were delineated back to 1200 CE using the annual dust peaks (Figures 2 and S1) which generally occur in spring. Infrequently when the dust signal below 90 m was less clear the $\delta^{18}O$ profile was consulted for assistance with annual layer counting. Above 90 m in the core this was not possible as sub-annual $\delta^{18}O$ variations likely reflecting individual precipitation events were more prominent (see the 60 – 90 meter section in Figure 2). Below ~100 meters the seasonal variability of $\delta^{18}O$ was a bit more prominent with the spring dust peak fairly well-aligned with the winter $\delta^{18}O$ minimum (Figure S1).

This smoothing of high frequency (sub-annual) $\delta^{18}O$ variations results from isotopic diffusion which typically occurs most rapidly in the upper, less dense firn layers that allow

the stable water isotopes in the firn air to mix with snow grains (Johnsen, 1977). Typically this smoothing allows seasonal variations in $\delta^{18}O$ to be more easily discerned although continued diffusion over much longer time periods will significantly dampen and eventually obliterate the annual signal (Johnsen, 1977; Johnsen et al., 2000). Moreover, differing isotopic diffusion factors for $\delta^{18}O$ and δD result in stronger smoothing of $\delta^{18}O$ than of δD which in turn may create an artificial annual cycle in the deuterium excess ($d_{ex} = \delta D - 8 \cdot \delta^{18}O$) (Dansgaard, 1964; Johnsen et al., 2000). This is not relevant here as we only used the $\delta^{18}O$ profile, not the d_{ex} profile.

Typically if the diffusion length at the drill site is small relative to the annual layer thickness then the impact of diffusion on the annual $\delta^{18}O$ signal should be minimal. The diffusion length depends on the accumulation rate, and the temperature and density profiles (Laepple et al., 2018). Examination of the literature reveals that diffusion lengths at 10 m depth on the very cold (-55^{0}C) and dry East Antarctic Plateau vary from ~0.05 to 0.08 m (Laepple et al., 2018, Figure 2). Johnsen et al. (2000) calculated the varying diffusion lengths over depths of 0 to 140 meters at Dome C, East Antarctica (-55^{0}C) and at the Summit Site in Central Greenland (-31.6^{0}C). Maximum diffusion lengths were found between 20 to 40 meters depth and varied from 0.06 to 0.10 meters. These sites are colder than B-C and have much lower accumulation rates. A more comparable site is the Renland ice cap in eastern Greenland (Holme et al., 2019) where the annual surface temperature is -18^{0}C and annual accumulation is ~ 0.47 m ice equivalent (0.43 m w.e.). Here the maximum modeled diffusion length of ~13 cm (density equivalent) occurs at ~25 to 30 m depth. Thus, the diffusion length on the B-C ice field is likely in the range of 0.10 to 0.15 m (w.e.) which implies that each water molecule moved a maximum of 0.15 m from its original stratigraphic position. This distance is very small relative to the average annual accumulation (1.38 m w.e. or ~2.13 m of snow using the mean density of 0.648) from 1971 to 2000 and suggests that diffusional smoothing of $\delta^{18}O$ over much of the B-C ice core is limited primarily to the reduction of sub-annual variability. It is also fortunate that the annual layer counting upon which most of the B-C core dating relies is highly dependent on insoluble dust which is a non-diffused parameter. The bottom ice may exceed 1500 years in age (Urmann, 2009), but this has yet to be confirmed by radiometric dating, geochemical analyses, and/or the identification of time-stratigraphic markers in the lowest 60 m of the core. This does not affect the data discussed in this paper which post-date 1200 CE.

Dating ice cores using annual layer counting is ideal for sites with clearly defined and well-understood seasonal variations in chemical or physical properties. This approach has been used successfully for cores from regions with both high (Goodwin et al., 2016) and low (Rasmussen et al., 2006) rates of accumulation. Layer counting approaches benefit from higher rates of accumulation, the use of multiple seasonally varying parameters, and

the identification of known time horizons such as elevated concentrations of excess sulfate that are typically associated with volcanic emissions. The high accumulation (1.38 m w.e.) on Bona-Churchill, the distinct seasonality in the deposition of insoluble (mineral) dust, and excellent preservation of the elevated concentrations of excess sulfate associated with a number of well-dated volcanic events facilitated the construction of a well-dated ice core record. Of course errors arise from a number of sources (see Rasmussen et al. (2006) for an excellent summary) but the largest contribution to dating uncertainty comes from erroneous interpretation of the annual layers. The assessment of dating errors in the last 800 years of the B-C core is discussed below using previously reported volcanic events. This discussion assumes that the date of a previously published volcanic event is accurate and that the temporal difference in the B-C core reflects errors in our layer counting. These errors vary from 0 to 4 years for the different core sections between consecutive volcanic events. As the errors for specific sections can be positive (too old) or negative (too young) it is the cumulative error at the bottom of the record that is of most interest. As discussed below, the cumulative error ranges from a few years to a maximum of 9 years depending on the correct year for the eruption of Katla whose published dates vary from 1179 to 1171 CE.

Figure S1 illustrates the 1900 to 1920 CE section of the B-C core that contains the well-documented June 6, 1912 eruption of Novarupta on the Aleutian Peninsula which is evident in the 1912 and 1913 snowfall characterized by elevated concentrations of excess sulfate (EXS, calculated using the Na^+ concentration to remove the sea salt contribution). Using EXS to identify specific volcanic eruptions in the B-C core is not as straightforward as in the polar ice sheets due to frequent eruptions of local and regional volcanoes in this tectonically active area where the history of such eruptions is incomplete. However, EXS concentrations associated with large, well-documented tropical and Northern Hemisphere volcanic eruptions are quite prominent and useful in confirming the dating and estimating the timescale error at specific depths. For example, the elevated EXS appearing in 1816 CE (Figure S2a) is almost certainly associated with the eruption of Tambora (1815 CE) while the elevated EXS appearing in 1810 CE is contemporaneous with an unidentified, but well-established, eruption in 1809 CE whose EXS is found in 1810 CE in both polar ice sheets (Dai et al., 1991).

A large EXS event in the B-C core (296 ppb) is dated as 1786 CE (Figure S2b) just three years later than the very well-documented eruption of Laki (Iceland), one of the largest eruptions in the Holocene, which left a distinct sulfate layer that is detected in all Greenland ice cores (Clausen et al., 1997). This suggests the possibility of a 3 year error in the B-C timescale at this depth. Another prominent volcanic signal found in ice cores in central and northern Greenland is dated at 1601 CE in the GRIP ice core (Clausen et al., 1995) and at 1603 CE in the GISP2 ice core (Zielinski, 1995; de Silva & Zielinski, 1998), both

in central Greenland. Clausen et al. (1995) suggest an eruption site in the high northern latitudes or the Alaska region but Zielenski (1995), among others, attribute it to the well-documented 1600 CE eruption of Huaynaputina in southern Peru. Figure S2c illustrates a very high EXS concentration dated as 1605 CE in the B-C core which suggests a possible timescale error up to ~4 years at this depth.

Fisher et al. (2004) report that the largest sulfate peak in the Eclipse and Mt. Logan cores occurs in 1516 CE. The largest EXS event in the B-C core (638 ppb) occurs in 1513 CE (Figure S2d), suggesting strongly that they share an identical source although the specific volcano has not been identified. These data suggest that the likely timescale error for this section of the B-C core is in the range of 3 years. Another prominent sulfate peak dated at 1179 CE in the GRIP core (Clausen et al., 1997) is attributed to the eruption of Katla (Iceland). In the B-C core a broad elevated peak in EXS is dated as 1170 to 1172 CE (Figure S2e). Mosley-Thompson et al. (2001) identified a similar sulfate peak at 1171 CE in the 1995 Humboldt ice core (Greenland) and more recently Sigl et al. (2015) produced a revised volcanic timescale that assigns a date of 1171 CE to this non-sea-salt sulfur peak in the NEEM (Greenland) ice core. Thus the estimated timescale error at this depth in the B-C core (403.1 m) is likely only one or two years although a maximum error of 9 years is possible depending on the "actual" data of the Katla eruption.

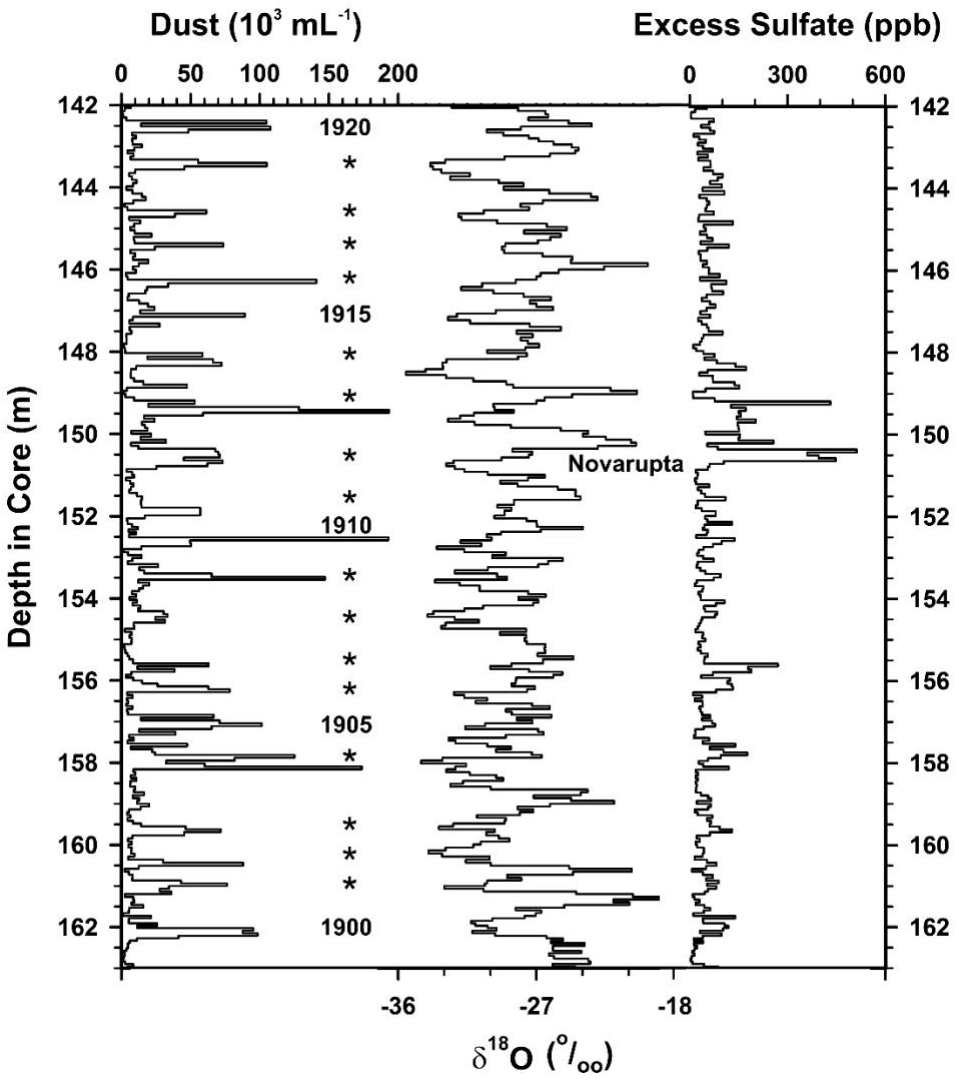

Figure S1. Timescale development for B-C ice core. Individual sample values for insoluble dust content, $\delta^{18}O$, and EXS are shown in the ice core section from 142 to 163 m depth that is dated from 1900 to 1920 CE using seasonal variations in dust content. Seasonal variations in $\delta^{18}O$ are more apparent in the core at some times than others, making it a less reliable dating tool. The 1912-13 EXS peaks are associated with the 1912 eruption of Novarupta.

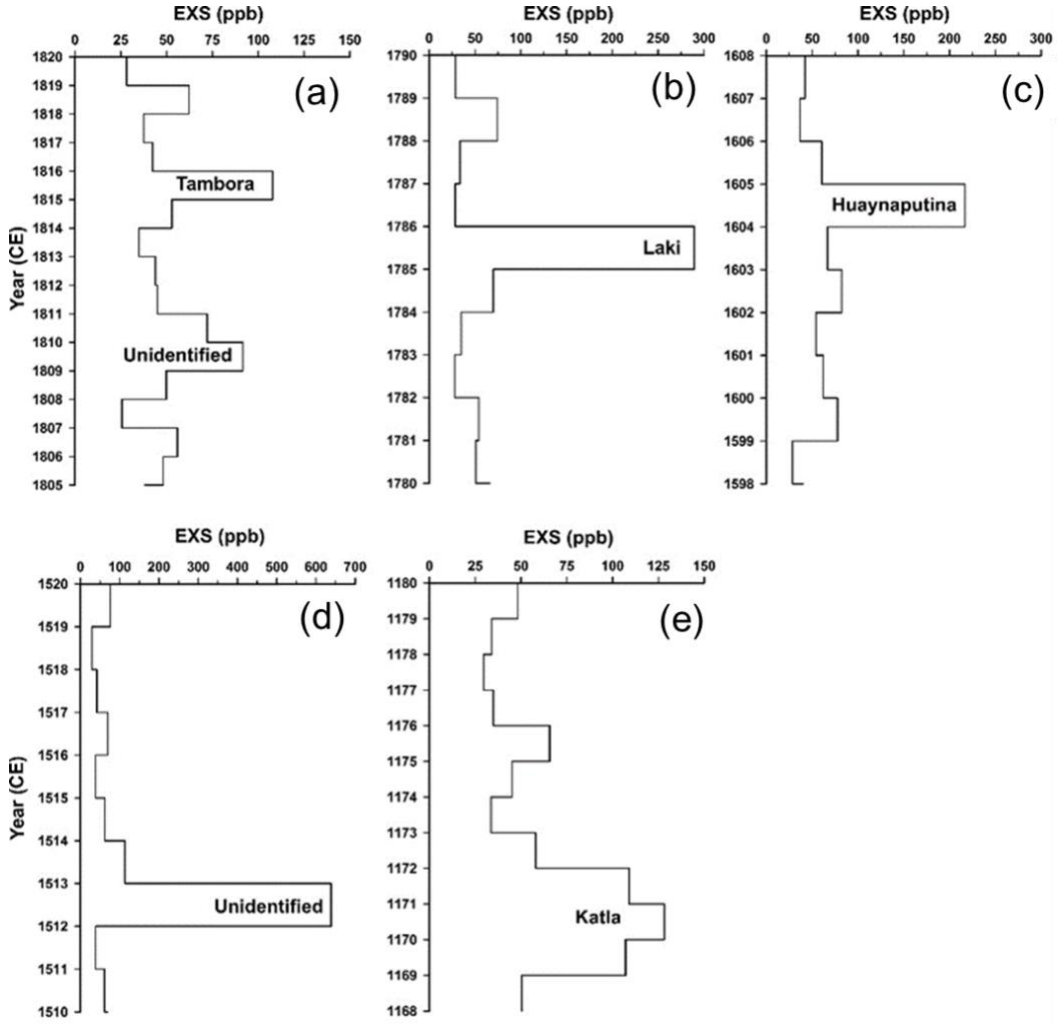

Figure S2. Various volcanic markers in five sections of the B-C ice core. Annual EXS concentrations represent volcanic events previously documented in other polar or high latitude ice core records as discussed in Text S1.

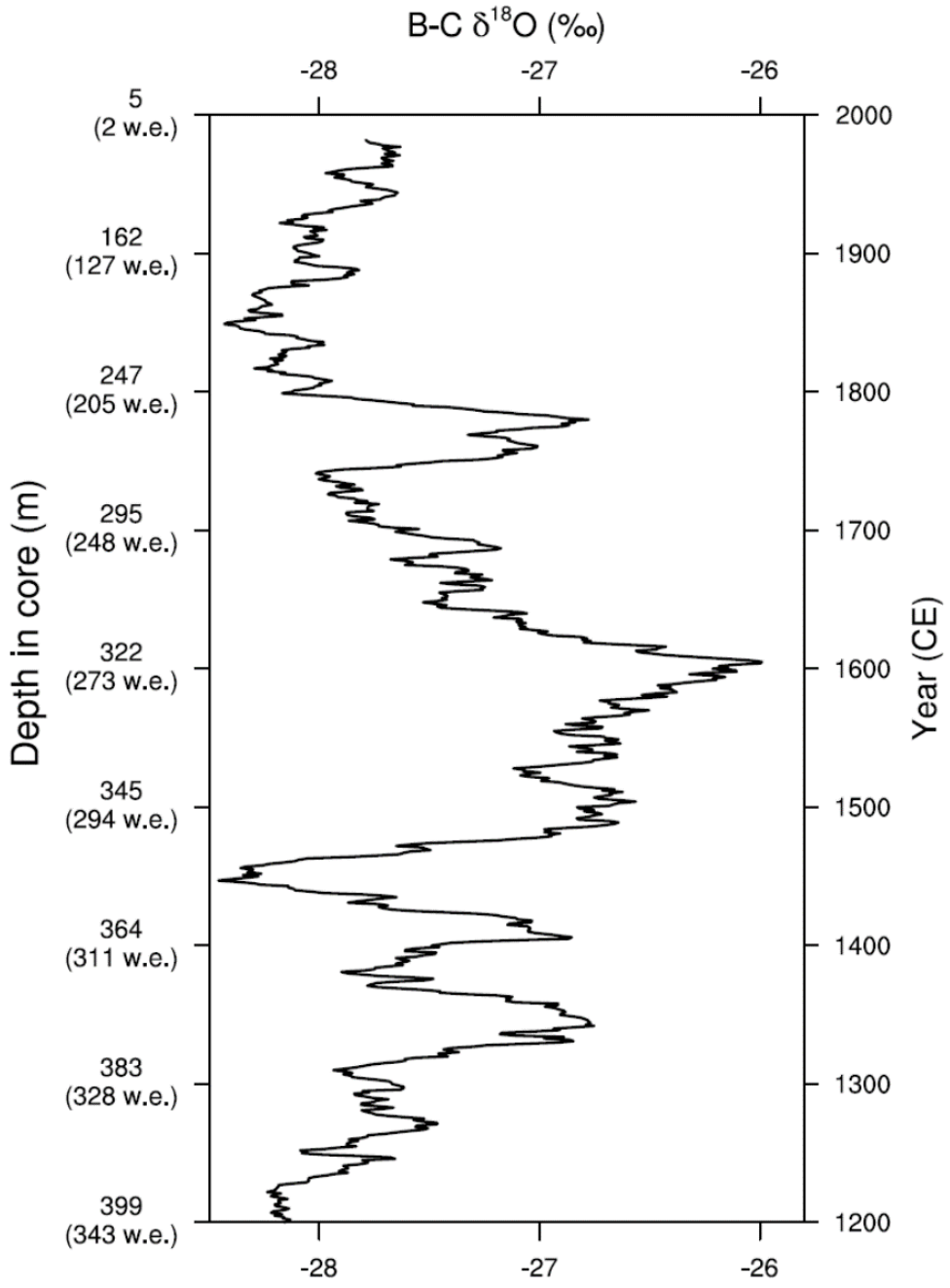

Figure S3. The 800-yr B-C $\delta^{18}O$ profile shown with respect to age (right axis) and depth in core (m and m w.e.; left axis).

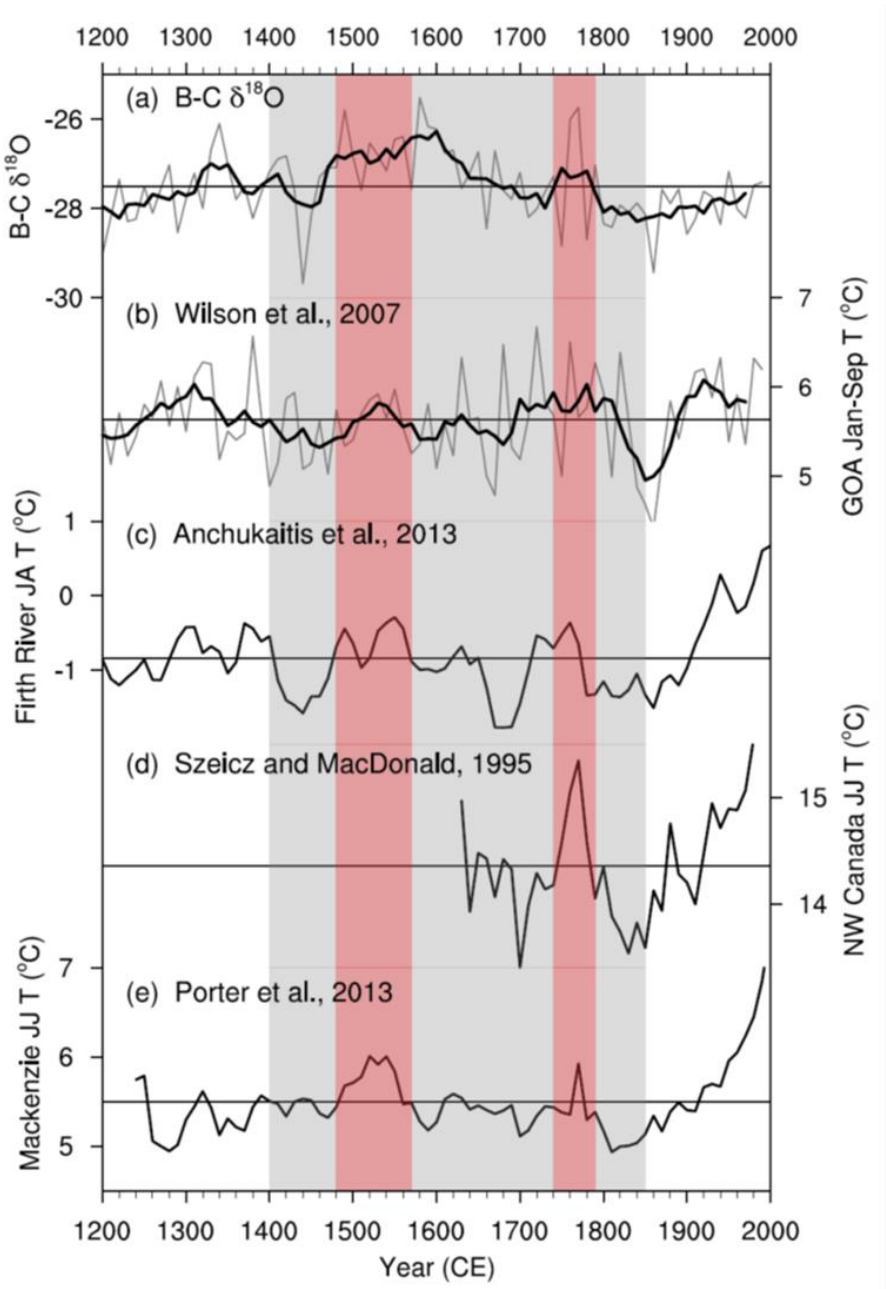

Figure S4. B-C $\delta^{18}O$ and tree ring-derived temperature reconstructions. (a) B-C $\delta^{18}O$ decadal averages (gray line) with 5-decade running means (black line), (b) Gulf of Alaska (GOA) January to September temperature reconstruction (Wilson et al., 2007), (c) July-August temperature reconstruction from the Firth River region (Anchukaitis et al., 2013), (d) June-July temperature reconstruction from NW Canada (Szeicz & MacDonald, 1995), (e) June-July temperature reconstruction from Mackenzie River Delta (Porter et al., 2013). Gray shading indicates the LIA period ~1400-1850 CE. The time intervals containing brief LIA warm periods (1490-1570 CE; 1740-1790 CE) are highlighted in pink.

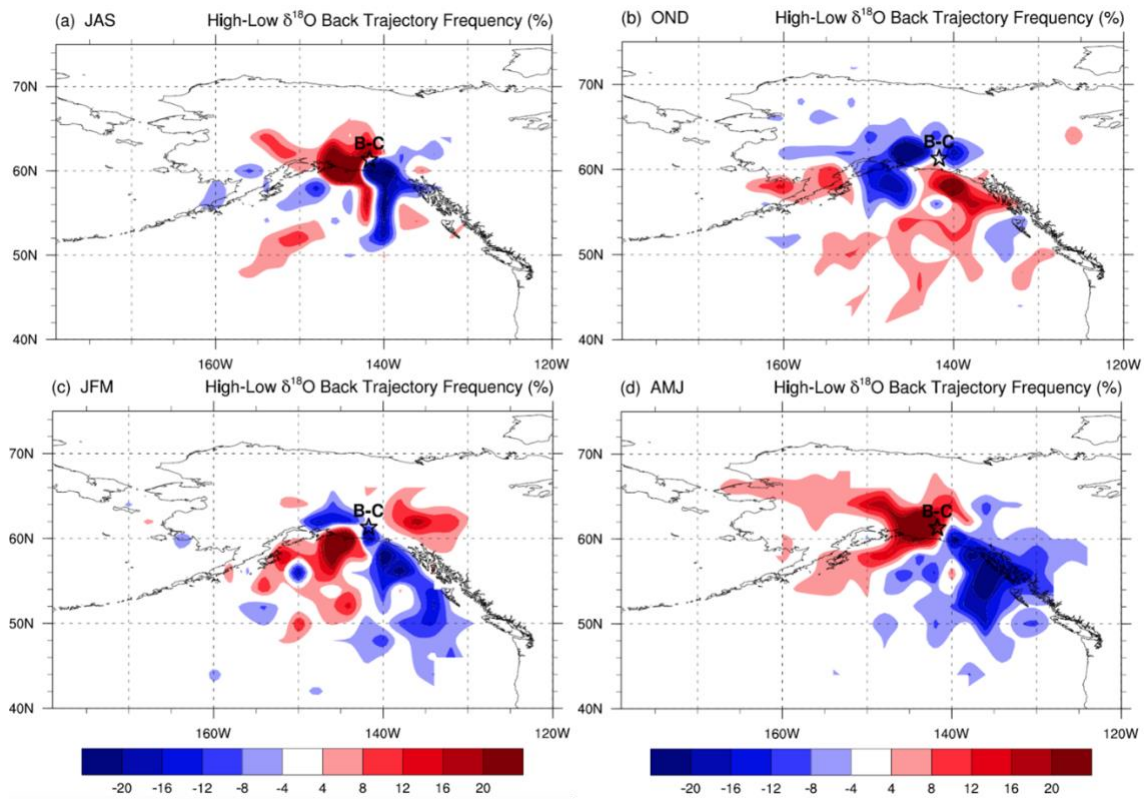

Figure S5. The difference in NOAA HYSPLIT back trajectory frequencies between the five highest and five lowest years of B-C $\delta^{18}O$ for each season during the 1979-2001 CE period.

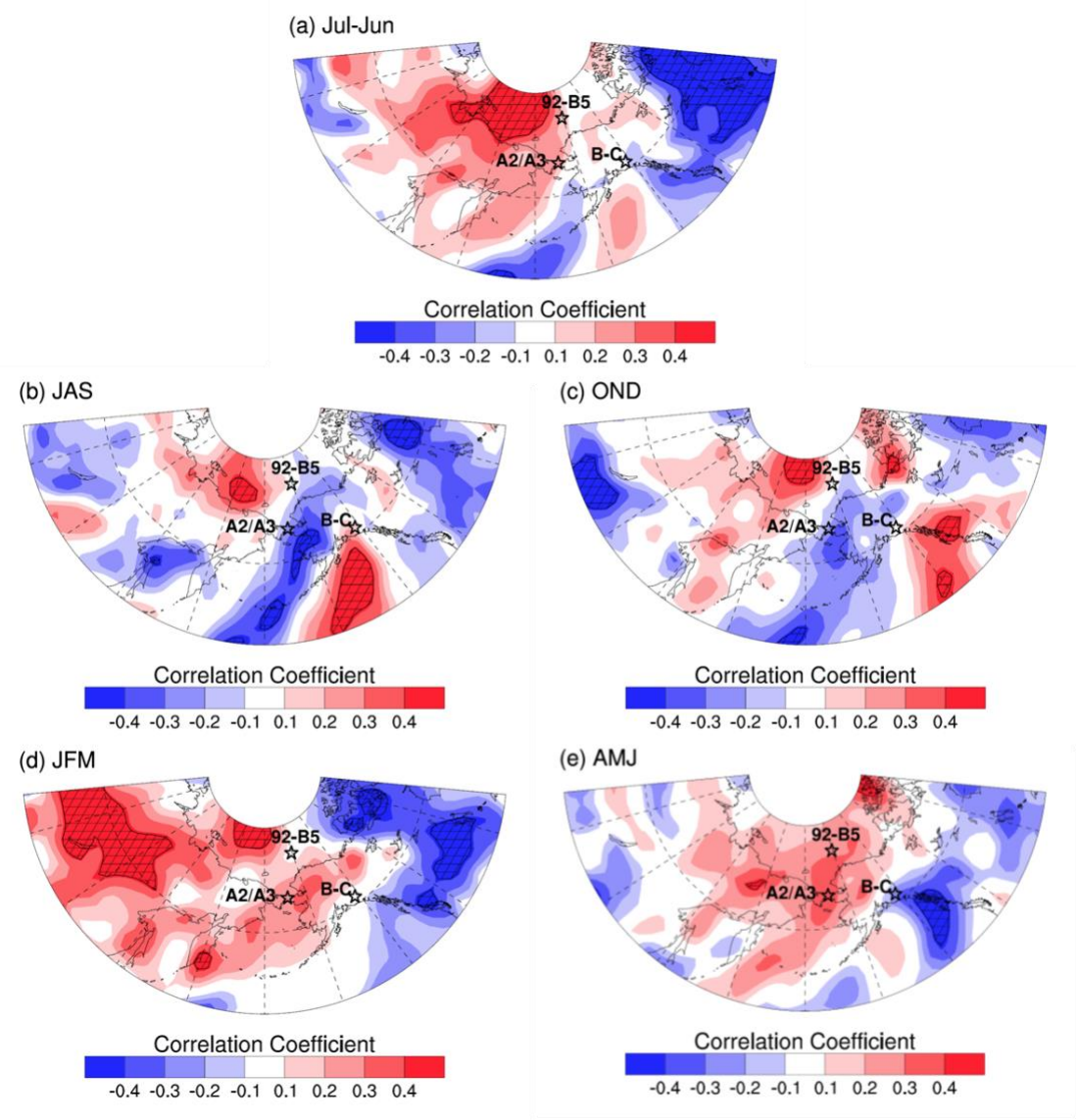

Figure S6. Spatial correlations between B-C $\delta^{18}O$ and 1000 hPa meridional wind (V) from 20th Century Reanalysis (Compo et al., 2011) for each season for the 1979-2001 CE period. Cross-hatching indicates 95% significance. Stars indicate the B-C site, A2/A3 moorings, and sediment core (92-B5) location.

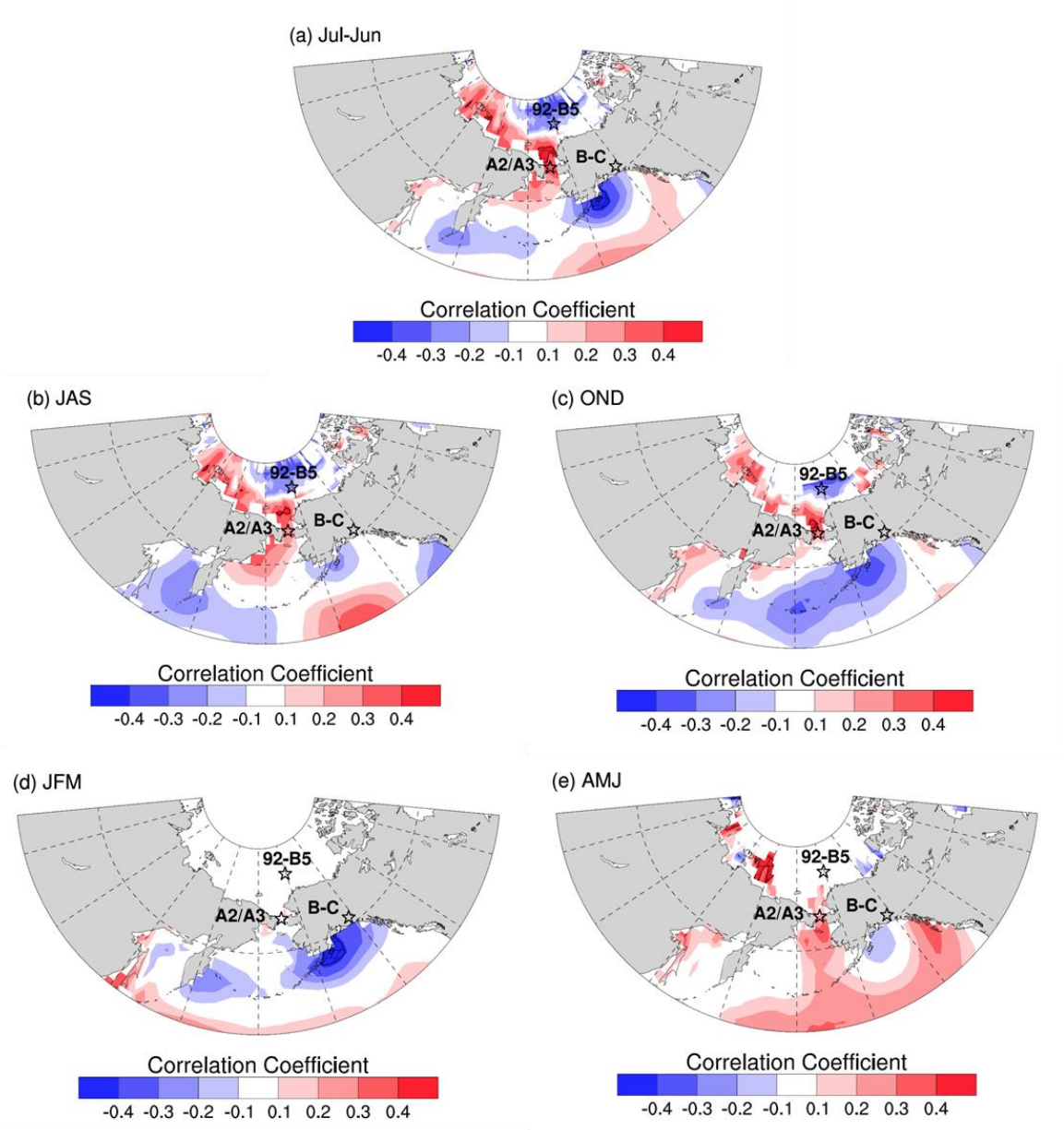

Figure S7. Spatial correlations between B-C $\delta^{18}O$ and SSTs from NOAA's extended reconstructed sea surface temperatures (Huang et al., 2015, 2016; Liu et al., 2015) for each season for the 1979-2001 CE period. Cross-hatching indicates 95% significance. Stars indicate the B-C site, A2/A3 moorings, and sediment core (92-B5) location.

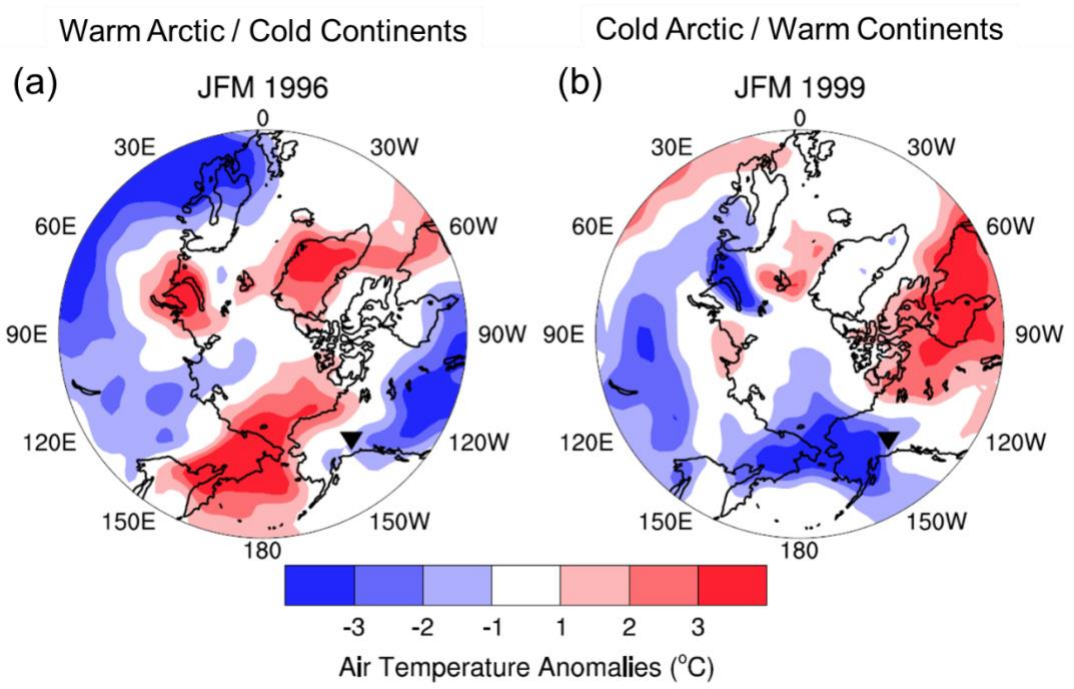

Figure S8. Temperature anomalies preceding two Western Arctic extremes. 1000 hPa winter (JFM) temperature anomalies for (a) 1996 and (b) 1999. Anomalies are relative to the 1981-2010 base period. These winters precede examples of warm/reduced sea ice and cold/enhanced sea ice conditions in spring (AMJ), respectively, as illustrated in Figure 7.

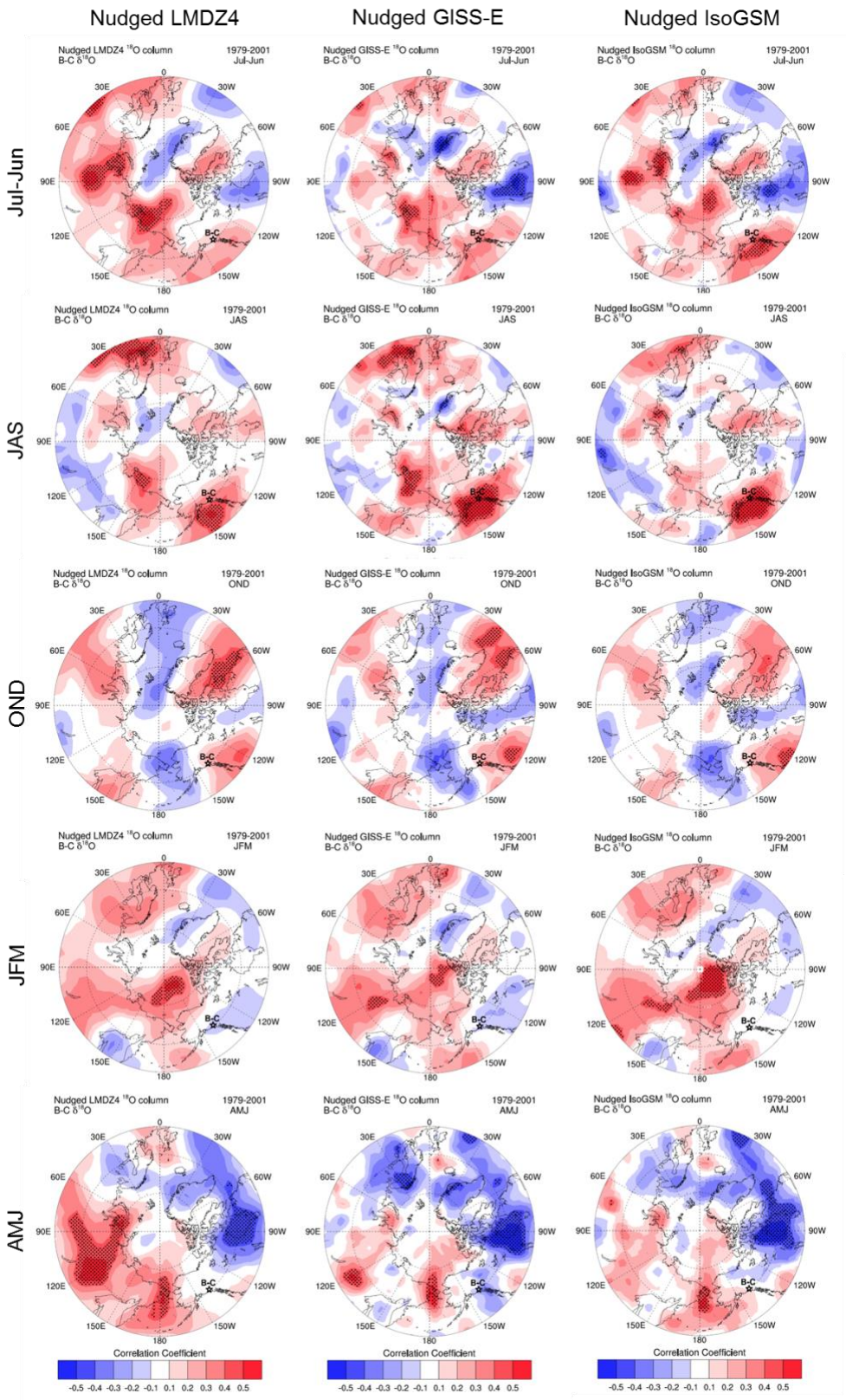

Figure S9. Spatial correlations between nudged modeled total column ^{18}O and annual B-C $\delta^{18}O$ for each season in the 1979-2001 period. Stippling indicates 95% significance.

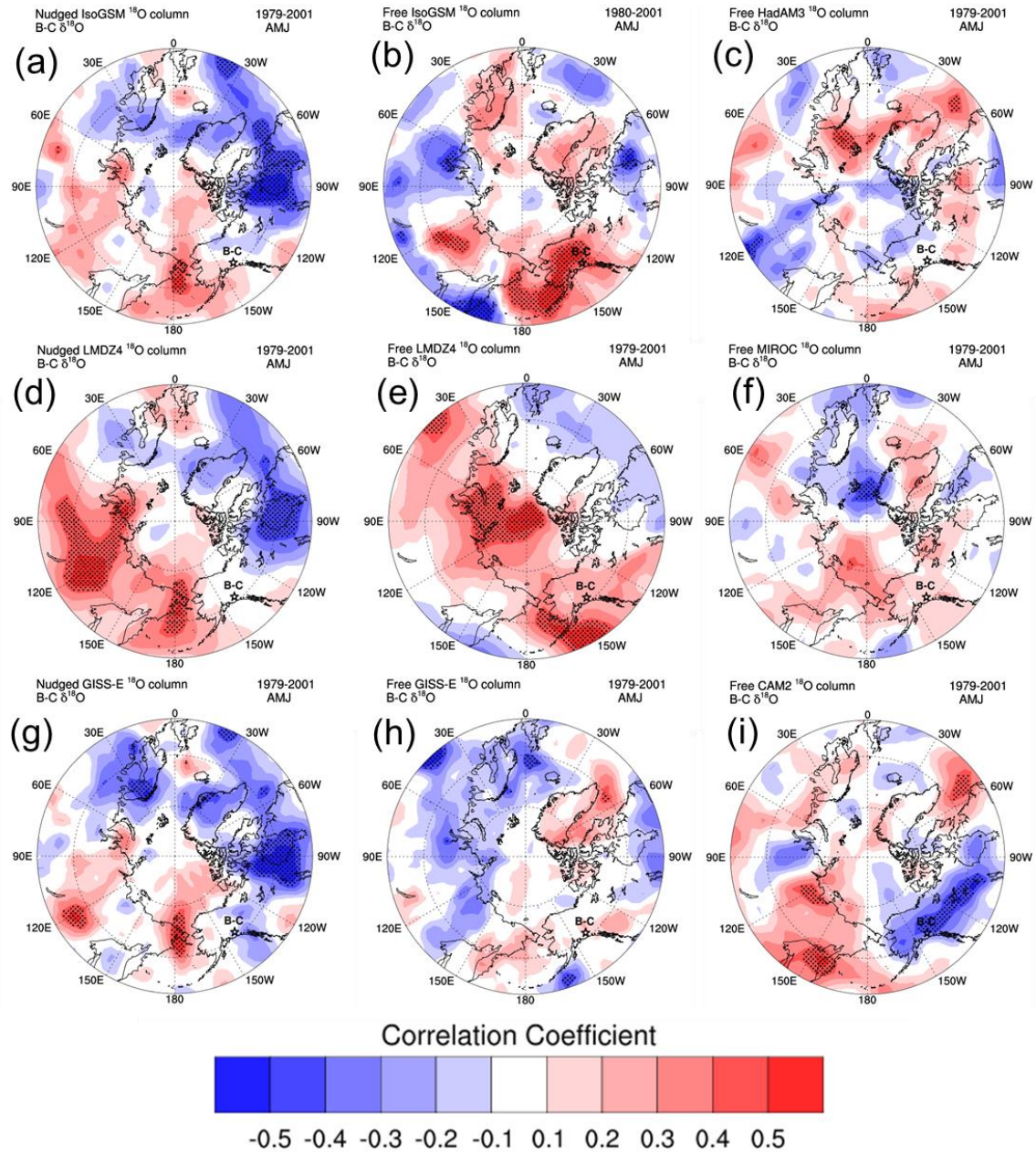

Figure S10. Spatial correlations between modeled total column ^{18}O in spring (AMJ) and annual B-C $\delta^{18}O$ for the 1979-2001 period. Stippling indicates 95% significance. Isotope-enabled model data were obtained from https://data.giss.nasa.gov/swing2/.

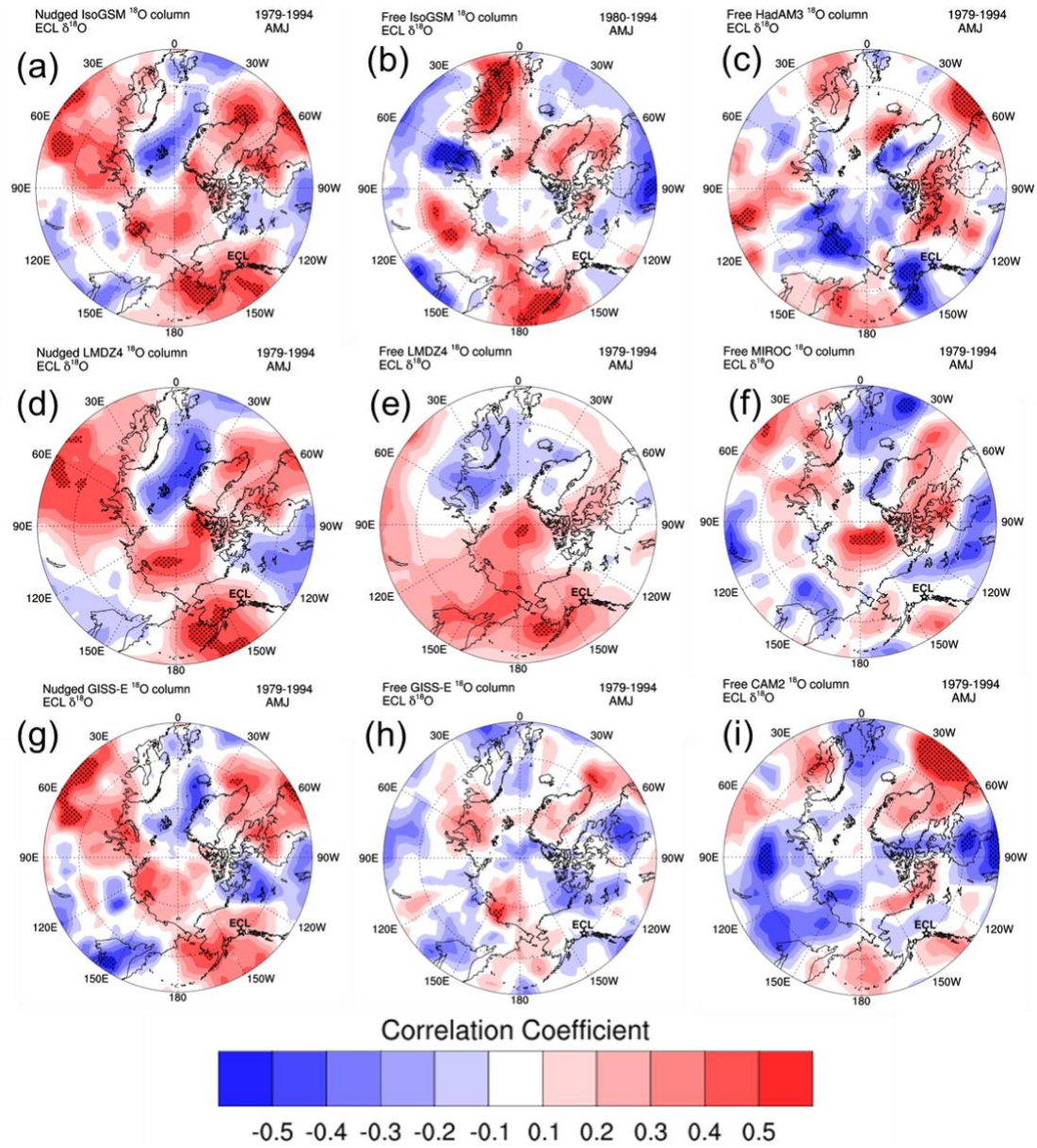

Figure S11. Same as Figure S10, but for Eclipse $\delta^{18}O$

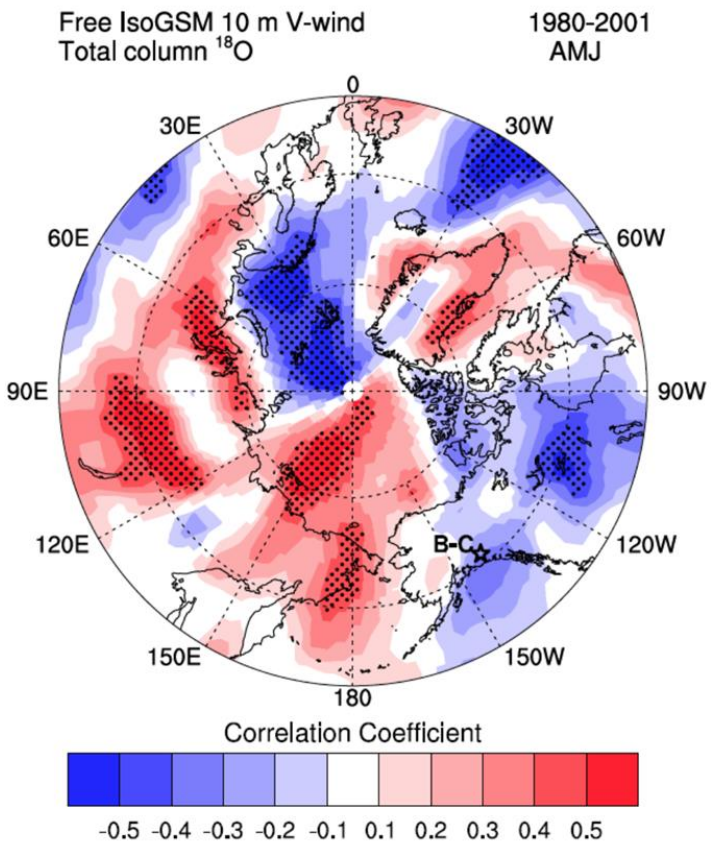

Figure S12. Spatial correlations between modeled AMJ ^{18}O over the B-C grid cell and gridded meridional winds from the free-running IsoGSM model (Yoshimura et al., 2008). Stippling indicates 95% significance.

Table S1. Metadata for meteorological stations in southeast Alaska (local) and along the western coast of Alaska. Climate divisions are by Bieniek et al. (2012).

Local Stations							
Name	**Latitude**	**Longitude**	**Elevation**	**Average T (°C)**	**Total P (inch)**	**Climate Division**	**Time span**
Cordova	60.48	-145.45	9.4 m	4.2	103.7	NE Gulf	1910-2001
Yakutat	59.51	-139.67	10.1 m	4.3	142.5	NE Gulf	1918-2001
McCarthy	61.42	-143.00	381.0 m	-1.5	19.0	SE Interior	1969-2001
Kennecott	61.48	-142.88	673.9 m	-0.9	22.6	SE Interior	1918-1947
McKinley Park	63.72	-148.97	630.9 m	-2.8	15.0	SE Interior	1923-2001
Gulkana	62.16	-145.46	476.1 m	-2.6	11.1	SE Interior	1943-2001
Matanuska	61.57	-149.25	52.4 m	2.0	15.3	Cook Inlet	1918-2001
Seward	60.13	-149.42	6.7 m	4.3	68.7	NW Gulf	1910-2001
Western Stations							
Name	**Latitude**	**Longitude**	**Elevation**	**Average T (°C)**	**Total P (inch)**	**Climate Division**	**Time span**
Bethel	60.79	-161.83	31.1 m	-1.5	17.2	West Coast	1924-2001
Kotzebue	66.87	-162.63	9.1 m	-5.8	9.2	West Coast	1941-2001
Nome	64.51	-165.44	4.0 m	-3.3	16.8	West Coast	1907-2001

Table S2. Metadata for isotope-enabled models

Model	**Reference**	**Simulations**	**Resolution**
IsoGSM	Yoshimura et al. (2008)	Free and nudged with NCEP	1.9° x 1.9°
GISS	Schmidt et al. (2007)	Free and nudged with MERRA	2° x 2.5°
LMDZ4	Risi et al. (2010)	Free and nudged with ECMWF	2.5° x 3.75°
CAM2	Lee et al. (2007)	Free	2.8° x 2.8°
HadAM3	Sime et al. (2008)	Free	2.5° x 3.75°
MIROC	Kurita et al. (2011)	Free	2.8° x 2.8°

Table S3. Correlation coefficients between annual B-C $\delta^{18}O$ and individual meteorological station temperatures. 3-yr running means of annual, seasonal, and post-

1950 spring (AMJ 50) temperature correlations are included. Bold indicates 95% significance.

Local Stations		ANN	JAS	OND	JFM	AMJ	AMJ 50
Cordova	1910-2001	-0.052	-0.063	-0.113	-0.088	0.092	0.179
Gulkana	1943-2001	0.119	**0.295**	0.149	-0.096	**0.361**	**0.356**
Kennicott	1918-1947	0.179	0.075	-0.019	-0.092	0.005	-
Matanuska	1918-2001	-0.050	-0.036	0.031	-0.197	0.201	**0.386**
McCarthy	1969-2001	0.254	0.056	0.066	0.217	0.286	0.286
McKinley Park	1923-2001	**-0.231**	-0.194	-0.102	-0.149	-0.168	0.070
Seward	1910-2001	-0.190	-0.041	-.125	**-0.233**	0.057	0.162
Yakutat	1918-2001	0.171	**0.444**	**0.320**	-0.050	0.127	**0.445**
Western Stations		**ANN**	**JAS**	**OND**	**JFM**	**AMJ**	**AMJ 50**
Bethel	1924-2001	0.161	**0.260**	0.113	-0.002	0.188	**0.423**
Kotzebue	1941-2001	0.185	0.074	-0.023	0.044	**0.298**	**0.345**
Nome	1907-2001	0.119	0.127	0.019	0.009	**0.269**	**0.512**

Table S4. Local meteorological station temperature correlations with B-C $\delta^{18}O$ for 1910-2001. Asterisks indicate 95% significance.

		Local Meteorological Station Temperature Data				
		Annual	JAS	OND	JFM	AMJ
B-C isotopes	Annual	-0.06	0.12	0.02	-0.08	-0.19
	3yr r. m.	-0.08	0.10	-0.06	-0.14	0.05

Table S5. Western Alaska meteorological station temperature correlations with B-C $\delta^{18}O$ for 1908-2001 and 1950-2001. Asterisks indicate 95% significance.

			Western Alaska Meteorological Station Temperature Data				
			Annual	JAS	OND	JFM	AMJ
B-C isotopes	1908-2001	Annual	0.09	0.15	0.03	0.03	0.12
		3yr r. m.	0.11	0.29*	-0.05	0.01	0.27*
	1950-2001	Annual	0.02	0.10	0.01	-0.02	0.05
		3yr r. m.	0.22	0.11	0.03	0.05	0.45*

Table S6. Correlation coefficients between Western Arctic sea ice area, A2/A3 mooring temperatures, and B-C $\delta^{18}O$. Asterisks indicate 95% significance.

		Western Arctic Sea Ice Area				
		Annual	JAS	OND	JFM	AMJ
B-C Isotopes	1979-2001	-0.16	-0.14	-0.02	0.03	-0.46*
A2/A3 Mooring	1991-2016	-0.67*	-0.25	-0.49*	-0.44*	-0.73*
		A2/A3 Mooring Data				
		Annual	JAS	OND	JFM	AMJ
B-C Isotopes	1991-2001	-0.32	-0.58	-0.09	0.39	0.70*

Table S7. Correlation coefficients among northwestern North American annual ice core records. Correlations in parentheses are for 3-yr running means. Asterisks indicate 95% significance.

	B-C $\delta^{18}O$	**Eclipse $\delta^{18}O$**	**Mt. Logan $\delta^{18}O$**
Eclipse $\delta^{18}O$	0.21* (0.48*)		
Mt. Logan $\delta^{18}O$	0.20 (0.15)	0.09 (0.14)	
Mt. Hunter Na^+	-0.21* (-0.18)	-0.02 (-0.13)	-0.09(-0.11)

Table S8. Correlations between modeled annual ^{18}O over the B-C grid cell and B-C $\delta^{18}O$. Ensembles include one using all of the models (all-model) and a subset with models in which correlations with B-C $\delta^{18}O$ exceed 0.2 (subset ensemble). Asterisks indicate 95% significance.

Model	**Correlation coefficient with B-C $\delta^{18}O$**
IsoGSM Free[†]	0.26
IsoGSM Nudged[†]	0.28
GISS Free	0.19
GISS Nudged[†]	0.28
LMDZ4 Free[†]	0.34
LMDZ4 Nudged	0.18
CAM2	-0.17

HadAM3[†]	0.20
MIROC	0.08
All-model Ensemble	0.31
Subset Ensemble	0.46*

[†]model included in subset ensemble